Atmospheric Environment 198 (2019) 34–45

Contents lists available at ScienceDirect

Atmospheric Environment

journal homepage: www.elsevier.com/locate/atmosenv

Emissions of nitrous oxide from continuous permafrost region in the Daxing'an Mountains, Northeast China

Weifeng Gao[a], Yunlong Yao[b], Hong Liang[c,*], Liquan Song[a], Houcai Sheng[d], Tijiu Cai[d], Dawen Gao[a,c,**]

[a] Center for Ecological Research, Northeast Forestry University, Harbin, 150040, China
[b] College of Wildlife Resources, Northeast Forestry University, Harbin, 150040, China
[c] School of Environment, Harbin Institute of Technology, Harbin, 150090, China
[d] College of Forestry, Northeast Forestry University, Harbin, 150040, China

GRAPHICAL ABSTRACT

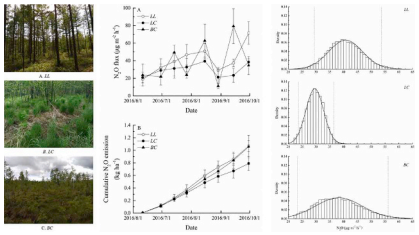

ARTICLE INFO

Keywords:
N_2O emission
Permafrost
Swamp forest
Environmental factors
Nitrate nitrogen
Daxing'an mountains

ABSTRACT

Permafrost ecosystems play an important role in global climate change, and climate warming would result in permafrost thawing and changing microbial mediated N cycles. Emissions of nitrous oxide (N_2O) are an important component of N budgets in high-latitude permafrost ecosystems, especially in the context of global climate change. However, few studies have investigated the emissions of N_2O from a swamp forest in a permafrost ecosystem. In this paper, we investigated the N_2O emissions rates and cumulative budget from continuous permafrost region in the Daxing'an Mountains, northeast China, and identified the key environmental factors affecting N_2O emissions from three swamp forests in the growing season. A bootstrapping model estimated that average N_2O fluxes during the growing season were 40.76 ± 6.13, 29.56 ± 3.21 and 38.27 ± 8.46 $\mu g\, m^{-2}\, h^{-1}$ from three swamp forests consisting of *Larix gmelinii - Ledum palustre var. dilatatum* (*LL*), *Larix gmelinii - Carex appendiculata* (*LC*) and *Betula fruticose - Carex schmidtii* (*BC*), respectively. The types of swamp forests had no statistically significant impact on N_2O emissions ($P > 0.05$). The cumulative N_2O emissions were estimated to be 1.07 ± 0.09 (*LL*), 0.79 ± 0.18 (*LC*) and 1.05 ± 0.11 $kg\, ha^{-1}$ (*BC*) in the swamp forests, indicating that the permafrost region of the Daxing'an Mountains might be a potential N_2O source during the growing season. The N_2O emissions were mainly controlled by soil temperature, water table level, pH, ammonium nitrogen, nitrate nitrogen, total organic carbon and the carbon-to-nitrogen ratio. N_2O emission showed significant negative correlation with nitrate nitrogen in the three swamp forests; thus, the low nitrate would limit the rate of N_2O emissions in the permafrost region. In addition, we found that denitrification could be the potential source of N_2O fluxes in the permafrost region of Daxing'an Mountains. Our results indicated that permafrost swamp forests were significant source for N_2O emissions, and N_2O emissions were controlled by multiple environmental factors.

* Corresponding author.
** Corresponding author. Center for Ecological Research, Northeast Forestry University, Harbin, 150040, China.
E-mail addresses: liangh119@hit.edu.cn (H. Liang), gaodw@hit.edu.cn (D. Gao).

https://doi.org/10.1016/j.atmosenv.2018.10.045
Received 24 January 2018; Received in revised form 21 October 2018; Accepted 23 October 2018
Available online 24 October 2018
1352-2310/ © 2018 Elsevier Ltd. All rights reserved.

1. Introduction

Nitrous oxide (N_2O) has a very strong global warming potential that is 265 times higher than that of carbon dioxide (IPCC, 2013). N_2O destroys the ozone layer by photochemical reaction, and is a more active and long-lived greenhouse gas than carbon dioxide and methane (IPCC, 2013; Ravishankara et al., 2009). According to the latest report from the Intergovernmental Panel on Climate Change, the recent (2011) atmospheric N_2O concentration reached 324 ppb, which was 20% higher than that in the pre-industrial revolution period (IPCC, 2013). Soils are the largest source of N_2O flux, accounting for approximately 60% of all N_2O emitted to the atmosphere (IPCC, 2013). In terrestrial systems, N_2O mainly originates from agriculture (fertilized) (Petersen et al., 2013; Qin et al., 2012; Verma et al., 2006), forest (Kiese et al., 2003; Tang et al., 2006; Yan et al., 2014) and grassland (Du et al., 2006; Li et al., 2015; Xu et al., 2003). In cold-climate terrestrial ecosystems, N_2O emissions have been neglected because nitrogen limitations in these ecosystems were thought to allow only negligible N_2O production (Cui et al., 2018; Gregorich et al., 2006; Köster et al., 2017; Ma et al., 2007; Palmer and Horn, 2012; Voigt et al., 2017a). However, high N_2O emissions have been found in the field permafrost peatland and tundra during the growing season (Marushchak et al., 2011; Mu et al., 2017; Repo et al., 2009).

The permafrost region, which occupies 25% of earth's terrestrial area and is mainly distributed in high-latitude and high-altitude areas. Permafrost soils are large C and N reservoirs. Hugelius et al. (2014) estimated SOC storage for the Northern circumarctic permafrost region is 1300 Pg with an uncertainty range of 1100–1500 Pg. Harden et al. (2012) estimated 31–102 (best estimate 66) Pg of total nitrogen at the top 3 m of permafrost soils. The thawing of permafrost could release large amounts of carbon and nitrogen via microbial decomposition, which would increase the global atmospheric budget for greenhouse gases (Harden et al., 2012; Schuur et al., 2009). The soils of permafrost region were characterized by cold temperatures and water-saturated; consequently, the soils of permafrost region have low availability of mineral nitrogen and low N mineralization rates (Siciliano et al., 2009). Mineral N, predominantly ammonium nitrogen (NH_4^+-N) and nitrate nitrogen (NO_3^--N), are the substrate for nitrification (the oxidation of ammonium to nitrite and then to nitrate, N_2O is produced as a by-product) and denitrification (the reduction of nitrate and nitrite to nitric oxide (NO), nitrous oxide (N_2O), and dinitrogen (N_2)) in soils, respectively (Butterbach-Bahl et al., 2013). In the subarctic permafrost peatlands, the N_2O fluxes could reach 31–31.4 mg m^{-2} day^{-1} during the growing season, which are as high as that of tropical rainforest (Marushchak et al., 2011; Repo et al., 2009). Recently, Repo et al. (2009) revealed that the bare peatland in the arctic region released N_2O emissions of approximately 0.1 Tg yr^{-1}, accounting for up to 0.6% of the global annual N_2O emission and indicating that permafrost region is a potential source of N_2O emissions.

Soil moisture and water table level had significant influence on the N_2O flux from permafrost region. The water table level was 18 ± 7 cm below soil surface and soil moisture was at 64% in the surface of peat circles, which were created both aerobic and anaerobic microenvironments that allow simultaneous aerobic nitrification and anaerobic denitrification to take place (Repo et al., 2009). The WFPS (water-filled pore space, 76% and 70% in 2007 and 2008, respectively, meanwhile the water table level was −17 ± 7 cm and −20 ± 11 cm) values for the peat circles were in the optimal range for N_2O production via denitrification (Marushchak et al., 2011). When the soil moisture was 130.9 ± 10.6% in the Qinghai-Tibetan Plateau, high N_2O flux is partially attributable to the relative high soil nitrogen contents (Mu et al., 2017). At the wet grassland, rapid mineralization of organic matter accumulated under waterlogged condition might supply inorganic nitrogen to the soil after flooding ended, which promoted high N_2O release (24–368 mg N_2O–N m^{-2} h^{-1}) under semi-waterlogged conditions (40–45%) (Takakai et al., 2008). When soil moisture was low in the permafrost region, which seemed be not beneficial to high N_2O released (Chen et al., 2017; Zhu et al., 2012). High N_2O emissions were mainly occurred in the simultaneously nitrification and denitrification or denitrification in the high soil moisture (Marushchak et al., 2011; Repo et al., 2009).

The N_2O emissions could come from nitrification, nitrifier denitrification and denitrification in one or more ways in the permafrost region (Gil et al., 2017; Gregorich et al., 2006; Ma et al., 2007; Marushchak et al., 2011). N_2O emissions were shown previously to be influenced by air temperature, soil temperature, water table level, soil moisture, pH, precipitation, NH_4^+-N, NO_3^--N, gross N mineralization, TOC, N content and C/N ratio (Chen et al., 2017; Cui et al., 2018; Gil et al., 2017; Ma et al., 2007; Marushchak et al., 2011; Paré and Bedard-Haughn, 2012). The N_2O emissions correlated positively with air temperature, soil temperatures, water table level and N content and a negative correlation with precipitation, pH, C/N ratio and SOM content at the subarctic permafrost region (Marushchak et al., 2011). N_2O fluxes from Great Hing'an Mountains positively correlated with soil temperature at 5, 10 and 15 cm depth, soil moisture at 10 cm depth and active layer depth (Cui et al., 2018). Soil temperature, moisture and their interaction could explain 9%, 9% and 8% of N_2O fluxes from Qinghai-Tibet Plateau, respectively (Chen et al., 2017). N_2O emissions were positively correlated with WFPS and C/N ratio at the soil surface in sub-Arctic permafrost peatlands (Gil et al., 2017). Daily N_2O emission rates were correlated with soil ammonium which exhibited a 4–9-fold decrease in concentration from Devon Island (Ma et al., 2007). Weak but significant positive correlations between N_2O emissions and soil gross N mineralization were observed for two permafrost ecosystems, suggesting that nitrifier denitrification is an active N pathway under field soil conditions (Paré and Bedard-Haughn, 2012). In contrast, at least one previous study showed that there was no significant correlation between N_2O flux and any of these environmental factors (Gregorich et al., 2006).

Permafrost region is extremely sensitive to climate change, and increased global temperature will cause thawing and degradation of the permafrost (Camill, 2005; Cheng and Wu, 2007). In the past 30 years, the average temperature has increased 0.6 °C in high-latitude regions, twice the global average increase (IPCC, 2013). Increasing global temperatures and consequent permafrost degradation will change N-cycle rates (Chen et al., 2012; Frey and McClelland, 2009), significantly affecting N_2O flux (Voigt et al., 2017b). Climate warming has been shown to increase the abundance of bacterial *amoA* and *nirK* genes and promote nitrification and denitrification, leading to a greater release of N_2O in the tundra permafrost region (Xue et al., 2016). By the end of this century, 29 Pg of permafrost N is projected to thaw and be released to the atmosphere (Harden et al., 2012).

Global warming has changed the soil microclimate and soil properties in the permafrost region. Changes in environmental factors affect the microbial community structure and diversity (Szukics et al., 2010; Yuan et al., 2018) and the nitrogen mineralization rate mediated by microorganisms (Bengtsson et al., 2003), which in turn change the N_2O gas emissions (Shvaleva et al., 2015). Nevertheless, there is uncertainty about the N_2O flux response to climate change in specific components of permafrost systems.

The Daxing'an Mountains are located in the southern margin of the Eurasian continent, which is the second largest permafrost region in China. The region is one of the most sensitive areas to climate change and the permafrost environment has been changed significantly since climate warming was first observed (Cheng and Jin, 2013; Jin et al., 2007). Over the past few decades to 2017, the average ground temperature of permafrost soil has risen by approximately 1.0 °C and the southern boundary has receded significantly northward by 50–150 km under the influence of climate warming, reducing the total area of permafrost region by approximately 35% (Jin et al., 2007). As a unique component of the cold environment, permafrost degradation has released large amounts of N to the atmosphere (Harden et al., 2012). N_2O

flux over the lifetime (114 yr^{-1}), could become as important as the climate–carbon cycle feedback caused by soil CO_2 release (Xu et al., 2012). In the past, N_2O studies on permafrost region have mainly focused on peatland and tundra ecosystems (Cui et al., 2018; Gil et al., 2017; Lamb et al., 2011; Marushchak et al., 2011; Palmer and Horn, 2012; Paré and Bedard-Haughn, 2012; Repo et al., 2009; Voigt et al., 2017a; Zhu et al., 2012). However, few studies have focused on N_2O flux in permafrost forest ecosystems, especially in northeast China.

We selected three types of swamp forests at a slope of mountain as our study sites. The three types of swamp forests were *Larix gmelinii - Ledum palustre var. dilatatum* swamp forest (*LL*), *Larix gmelinii - Carex appendiculata* swamp forest (*LC)* and *Betula fruticose - Carex schmidtii* swamp forest (*BC*), which had significant difference in the water table level (the water table level from low to high) and plant composition. The three type of swamp forests were typical and widely distribution in Daxing'an Mountains, which could representative the N_2O flux from permafrost region of Daxing'an Mountains. The objectives of this study were to: (i) understand the variation of N_2O flux and evaluate the average N_2O flux and cumulative budget during the growing season; (ii) the difference of N_2O flux between three types of swamp forests and their drivers; (iii) quantify the relationship between N_2O fluxes and environmental factors in the growing season; (iv) compare N_2O emissions from Daxing'an Mountains with the global permafrost region scale. Information from this study is important as a quantitative basis for estimating global or regional N_2O emission inventories.

2. Materials and methods

2.1. Study site

The study site was situated in the continuous permafrost region in the Heilongjiang Mohe Forest Ecosystem Research Station in the Daxing'an Mountains of northeast China (122°06′–122°27′E, 53°17′–53°30′N) (Fig. 1). The study area is characterized by a typical cold temperate continental monsoon climate with the mean annual air temperature of −4.9 °C. The mean annual precipitation is 430–550 mm, and 60% of the precipitation occurs as rainfall, which is mainly concentrated between July and August. In this region, snowpack covers the land more than half the year (from October to April). The frost-free period for plant growth spans 80–90 days, typically from May to September. The annual total solar radiation is 401.93–447.99 kJ cm^{-2} and annual sunshine hours are in the range 2377–2625 h, with accumulated temperature of 1436–2062 °C for days having a mean temperature ≥10 °C. The soil at the study site is predominantly brown coniferous forest soil, interspersed with meadow soil and marsh soil (Zhang, 2002). The soil type of our study plots was marsh. Soil physics (soil temperature, water table level and pH) and soil chemistry (NH_4^+-N, NO_3^--N, TOC, TN and C/N ratio) in the 0–20 cm depth during the growing season as shown in Table 1. The soil thawing begins in April, and the thaw depths reach their maximum in the middle of September.

The typical vegetation in this area is cool-temperate coniferous forest with the dominant species of *Larix gmelinii*. The swamp forests are classified into three types based on the dominant vegetation according to Lang (Lang (1999). *Larix gmelinii - Ledum palustre var. dilatatum* swamp forest (*LL*) was dominated by *Larix gmelinii* and *Ledum palustre var. dilatatum* interspersed with *Betula platyphylla*, *Betula fruticose*, *Vaccinium uliginosum* and *Vaccinium vitis-idaea*. *Larix gmelinii - Carex appendiculata* swamp forest (*LC)* was dominated by *Larix gmelinii* and *Carex appendiculata* interspersed with *Betula platyphylla*, *Betula fruticose* and *Alnus sibirica*. *Betula fruticose - Carex schmidtii* swamp forest (*BC*) was dominated by *Betula fruticose* and *Carex schmidtii*.

2.2. N_2O gas sampling and analysis

We used the static opaque chamber technique to measure N_2O fluxes (Hutchinson et al., 2000). In June 2016, three plots at each swamp forest (*LL*, *LC* and *BC*) were established permanently for measuring N_2O rates in the nature reserve of the Daxing'an Mountains. An open square-framed polypropylene base collar (50 cm × 50 cm × 20 cm high) with a groove in the upper edge (to serve as a water seal) was randomly located within each plot and permanently inserted 20 cm into the soil during the experimental period. During sampling, an open-bottom polypropylene chamber (50 cm × 50 cm × 50 cm) was placed on the pre-inserted base and used to collect N_2O from the soil.

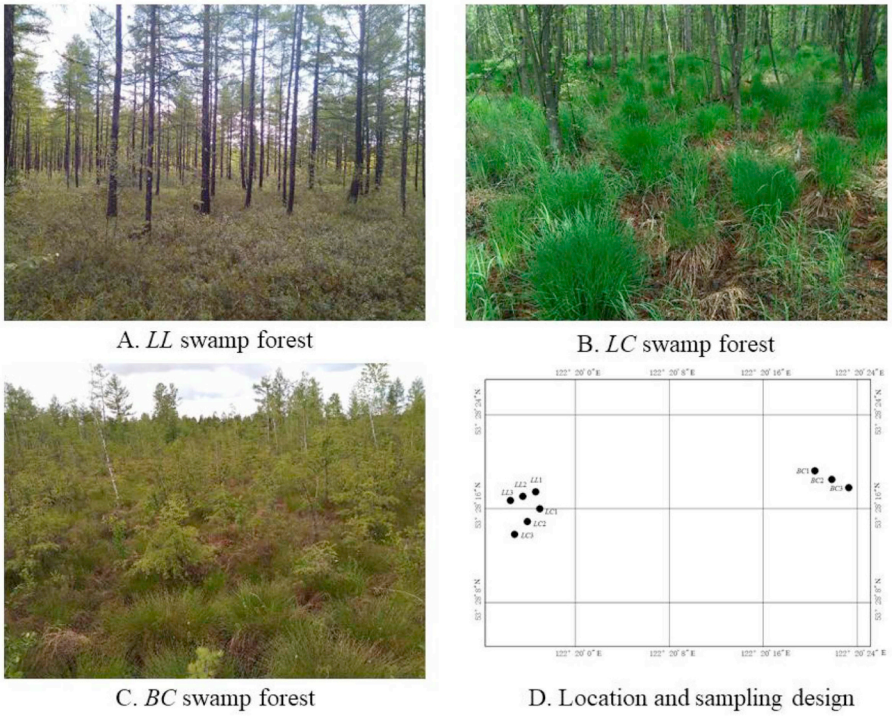

Fig. 1. Basic landcover in the study region (A, B and C) and the location and sampling design (D) of the three types of swamp forests in the Daxing'an Mountains, northeast China. Swamp forest types were *Larix gmelinii - Ledum palustre var. dilatatum* (*LL*), *Larix gmelinii - Carex appendiculata* (*LC*) and *Betula fruticose - Carex schmidtii* (*BC*).

Table 1
Physicochemical characteristics in the 0–20 cm depth of soil in the three swamp forests in the Daxing'an Mountains, northeast China (mean ± SD).

Plot	Soil temperature (°C)	Water table level (cm)	pH	NH_4^+-N (mg kg^{-1})	NO_3^--N (mg kg^{-1})	TOC (g kg^{-1})	TN (g kg^{-1})	C/N
LL	8.23 ± 2.98a	−13.14 ± 10.65b	4.68 ± 0.13c	4.38 ± 2.03a	0.86 ± 0.33a	53.41 ± 5.61b	3.01 ± 0.51b	17.72a
LC	8.02 ± 2.95a	−1.87 ± 4.87a	5.04 ± 0.11a	5.14 ± 1.52a	0.78 ± 0.33a	62.38 ± 3.80a	5.01 ± 0.50a	12.46b
BC	9.20 ± 2.51a	+2.59 ± 5.14a	4.87 ± 0.09b	4.22 ± 1.84a	0.80 ± 0.22a	49.42 ± 4.81b	2.51 ± 0.17c	19.68a

Different lowercase letters of a, b, and c within a column indicate significant differences ($P < 0.05$) among types of swamp forests at the Daxing'an Mountains, northeast China. In the column of water table level, "+/−" represent above or below soil surface. NH_4^+-N, ammonium nitrogen; NO_3^--N, nitrate nitrogen; TOC, total organic carbon; TN, total nitrogen; C/N, carbon-to-nitrogen ratio. Swamp forest types were *Larix gmelinii - Ledum palustre var. dilatatum* (*LL*), *Larix gmelinii - Carex appendiculata* (*LC*) and *Betula fruticose - Carex schmidtii* (*BC*).

Gas sampling to determine N_2O fluxes was carried out between 9:00 a.m. and 11:00 a.m. (Alves et al., 2012) on two occasions per month starting in June 2016 and ending in September 2016 (eight sampling events in total). A 50-ml plastic syringe equipped with a three-way stopcock was inserted in the sample connection of the chamber after water sealing. Air from inside a chamber was withdrawn at the beginning of an event and every 15 min thereafter over a 45-min period using the syringe (total of four samples each event). Samples were injected into 100-ml pre-evacuated gas sampling bags (Delin Gas Packing Co., Dalian, China) for subsequent laboratory analysis. Air temperature inside the chamber was measured when gas samples were being retrieved.

The concentrations of N_2O were analyzed with a gas chromatograph (Shimadzu GC2010, Shimadzu Analytical and Measuring Instruments Division, Kyoto, Japan) by the Northeast Institute of Geography and Agroecology, Chinese Academy of Sciences. Compressed air containing 0.378 ppm N_2O was used for calibration. N_2 was used as the carrier gas with a flow rate of 20 mL min^{-1}. The N_2O was separated using a 1-m stainless steel column with an inner diameter of 2 mm Porapak Q (80/100 mesh), and was detected by an electron capture detector. The temperature for gas separation was maintained at 70 °C, and the detector was set at 250 °C. Fluxes were determined using linear regression analysis of results from samples collected throughout the 45-min sampling period for each chamber.

2.3. Soil sampling and analysis

During gas sampling, soil temperature (ST) at 10-cm depth was measured in the vicinity of each chamber using a portable digital thermometer with a thermocouple probe (JM-624, Jinming Corp., Tianjin, China). The water table level (WTL) also was measured near the chamber in each plot using a ruler (Dobbie and Smith, 2006). Soil samples were collected at the depth interval of 0–20 cm and analyzed for pH, ammonium nitrogen (NH_4^+-N), nitrate nitrogen (NO_3^--N), total nitrogen (TN) and total organic carbon (TOC). At each swamp forest site, we collected a soil core (using a stainless steel corer 3.8 cm in diameter) from each of three randomly selected locations that were close to each collar. Fine roots and visible organic debris were removed by passing the soil samples through a 2-mm sieve. Then, samples were transported in an insulated box (Esky) and stored at 4 °C for subsequent chemical analysis.

Soil samples were air dried and passed through a 2 mm sieve for analyses of the soil pH determination. Soil pH was measured in a 2:5 air-dried soil: deionized water mixture using an InoLab pH meter (WTW InoLab pH 730, Weilheim, Germany). Soil inorganic N (NH_4^+-N and NO_3^--N) was extracted using 1 mol/L KCl by shaking for 1 h. The extracts were filtered through via 0.45 μm pore-diameter syringe filter, and then soil inorganic N were analyzed using a Lachat flow-injection auto-analyzer (Seal Analytical AA3, Norderstedt, Germany). For the analyses of total N and C, sub-samples were further ground to a fine powder (< 0.15 mm). Total N concentration was determined on aliquots of 1.0 g of soil using semi-micro-Kjeldahl method (Bremner and Mulvaney, 1982). The TOC content was determined by oxidation at 170 °C, with potassium dichromate in presence of sulphuric acid. The excess potassium dichromate was titrated with a solution of Mohr's salt (Nelson and Sommers, 1996).

2.4. Statistical analysis

The gas flux was calculated as reported by Song et al. (2008) and Song et al. (2009):

$$F = \frac{dc}{dt}\frac{M}{V_0}\frac{P}{P_0}\frac{T_0}{T}H$$

where F is the gas flux (μg m^{-2} h^{-1}), dc/dt is the slope of the linear regression for the gas concentration gradient over time (μmol mol^{-1} h^{-1}); M is the molecular mass of gas (g mol^{-1}); P is the atmospheric pressure (Pa); T is the mean value of the air temperature inside the chamber during sampling (K); V_0, T_0, and P_0 are the gas mole volume (m^3 mol^{-1}), absolute air temperature (K), and atmospheric pressure under standard conditions (Pa), respectively; and H is the effective height of chamber (m). Average gas flux and standard deviation were calculated from three replicates for all observations. Cumulative N_2O emissions were linearly and sequentially accumulated from the emissions between every two adjacent intervals of the measurements following the procedure of Ding et al. (2007).

We used bootstrapping to estimate the means of N_2O fluxes and confidence intervals from the three swamp forests and sampling times at all sites. For each type of swamp forest, fluxes were re-sampled with 10000 iterations across blocks to generate a normal distribution of mean fluxes. A one-way analysis of variance was used to test the difference of N_2O emissions and environment factors. The correlations of the N_2O fluxes with environmental factors were tested using correlation analysis and stepwise multiple linear regression analysis. R software (Version 3.4.1, https://www.r-project.org/) was used for the statistical analyses. Significance was analyzed using Fisher's least significant difference (LSD) test at a probability level of 95% ($P < 0.05$). All figures were drawn using OriginPro 2016 software (OriginLab Corp., Northampton, MA, U.S.A.).

3. Results

3.1. N_2O emissions

During the study period (June–September 2016), the three types of swamp forest surfaces showed positive N_2O fluxes (Fig. 2A). A large temporal variation in the N_2O fluxes was observed throughout the experiment for all swamp forests (Fig. 2A). The N_2O emissions from *LL* and *LC* plots had similar temporal variation. Flux of N_2O showed a gradual increasing trend from June to the middle of August, then decreased until 29 August, after which they increased to the end of the growing season in September. The highest N_2O flux from *LL* plots was observed on 30 September, but the peak flux from *LC* plots occurred much earlier on 15 August. The N_2O flux of the *BC* plots fluctuated and the peak appeared on 14 September.

The nitrous oxide fluxes ranged from 18.82 to 71.57 μg m^{-2} h^{-1} in

LL plots, from 20.86 to 39.41 μg $m^{-2} h^{-1}$ in *LC* plots and from 11.81 to 79.25 μg $m^{-2} h^{-1}$ in *BC* plots (Fig. 2A, Table 2). The mean values of N_2O fluxes were 40.74 ± 15.98 μg $m^{-2} h^{-1}$ (*LL*), 29.54 ± 7.28 μg $m^{-2} h^{-1}$ (*LC*) and 38.34 ± 23.42 μg $m^{-2} h^{-1}$ (*BC*), and there was no significant difference in the mean fluxes from the three types of swamp forests (Table 2). The temporal coefficient of variation (CV) of the N_2O fluxes was 40.74% (*LL*), 29.54% (*LC*) and 38.35% (*BC*) (Table 2). The observed N_2O fluxes were positive, so that the cumulative N_2O emissions continued to increase over time. The cumulative N_2O emissions were 1.07 ± 0.09, 0.79 ± 0.18 and 1.05 ± 0.11 kg ha^{-1} from *LL*, *LC* and *BC* plots, respectively (Fig. 2B).

3.2. N_2O emissions variations for different swamp forest types

The bootstrapping estimation showed that predicted N_2O emissions were generally normally distributed (Fig. 3). Significant N_2O fluxes were released from the three swamp forests ($P < 0.01$). The bootstrap estimates of N_2O emissions from the *LL* plots ranged from 29.47 to 53.73 μg $m^{-2} h^{-1}$ (± 95% confidence interval), with the mean of 40.76 ± 6.13 μg $m^{-2} h^{-1}$. N_2O fluxes from the *LC* plots ranged from 23.00 to 35.55 μg $m^{-2} h^{-1}$ (± 95% confidence interval), with the mean of 29.56 ± 3.21 μg $m^{-2} h^{-1}$. N_2O fluxes from the *BC* plots ranged from 23.25 to 56.15 μg $m^{-2} h^{-1}$ (± 95% confidence interval), with the mean of 38.27 ± 8.46 μg $m^{-2} h^{-1}$. The N_2O emissions were mainly distributed between 23.00 and 56.15 μg $m^{-2} h^{-1}$ from the active layer soil (Fig. 3). The distributions of N_2O fluxes from *LL* and *BC* plots had the similar central tendency (40.76 ± 6.13 and 38.27 ± 8.46 μg $m^{-2} h^{-1}$, respectively), but the distribution of N_2O fluxes form *LC* plots was concentrated around a mean of 29.56 μg $m^{-2} h^{-1}$, which was smaller than the mean fluxes from *LL* and *LC* (Fig. 3). The *LL* and *BC* plots had similar variability in N_2O emissions, and this variability was greater than for the *LC* plots.

3.3. Correlations between soil physicochemical characteristics and N_2O emissions

The swamp forest soils exhibited statistically significant differences in water table level, pH, TOC, TN and carbon-to-nitrogen (C/N) ratio (Table 1). The water table level was significantly lower at *LL* plots than at *LC* and *BC* plots. The pH was highest in the *LC* plots and lowest in the *LL* plots. The *LC* plots had higher TOC than *LL* and *BC* plots, but a lower C/N ratio. The TN was highest in the *LC* plots and lowest in the *BC* plots. There were no significant differences in soil temperature, NH_4^+-N and NO_3^--N in the three types of swamp forests (Table 1).

Table 3 summarizes the results of the Pearson's correlation analysis for the observed N_2O flux against various environmental factors. In *LL* plots, N_2O flux only exhibited a negative correlation with NO_3^--N ($P < 0.05$, Table 3). There was no significant correlation between N_2O flux with any environmental factors in the *LC* and *BC* plots.

Stepwise multiple linear regression was used to identify the key environmental factors affecting N_2O emissions. The results showed that soil temperature, water table level, pH, NH_4^+-N, NO_3^--N, TOC and C/N were the dominant factors controlling N_2O emissions from the three swamp forests in the growing season (Table 4). In the different types of swamp forests, the N_2O fluxes were influenced by different key environmental factors. In the *LL* plots, N_2O emissions had significant positive correlations with pH and NH_4^+-N and negative correlations with water table level and NO_3^--N ($P < 0.001$). In the *LC* plots, N_2O flux had significant positive correlations with soil temperature and C/N, and negative correlations with NO_3^--N and TOC ($P < 0.001$). In the *BC* plots, N_2O emissions had significant positive correlations with water table level and C/N, and negative correlations with NO_3^--N and TOC ($P < 0.05$). The environmental factors could explain 73.89%, 62.41% and 49.05% of the total variation in the N_2O fluxes from the *LL*, *LC*, *BC* plots, respectively.

4. Discussion

4.1. The Daxing'an mountains emitted intermediate levels of N_2O from the permafrost ecosystems

From a review of previous studies, scientists have conducted N_2O flux release studies in field permafrost region and soils of permafrost region. Approximately two-thirds of studies were done during the growing season in in-situ permafrost (Table 5), and one-third used incubated permafrost soil in the laboratory (Cui et al., 2016; Elberling et al., 2010; Palmer et al., 2012; Rodionow et al., 2006; Siciliano et al., 2009; Voigt et al., 2017b; Wang et al., 2014). The largest N_2O fluxes in Arctic ecosystems in situ have been found in peatlands, so it makes sense that these surface types are studied more intensively (Table 5). However, few studies focused on the N_2O emissions from field swamp forests in permafrost region.

The N_2O fluxes that we measured during the growing season from swamp forests in the continuous permafrost region of the Daxing'an Mountains ranged from 11.81 to 79.25 μg $m^{-2} h^{-1}$. The results were within the range of N_2O emissions reported by a number of similar studies in the permafrost ecosystems (−25–2662 μg $m^{-2} h^{-1}$, Table 5). Repo et al. (2009) and Marushchak et al. (2011) found that the rate of N_2O emission from peatlands in arctic permafrost region were ranged from 1297 to 1308 μg $m^{-2} h^{-1}$, which was similar to the N_2O emissions rate from tropical rain forest (1213 μg $m^{-2} h^{-1}$) (Castaldi et al., 2013). In the northern Qinghai-Tibetan plateau, the N_2O flux were ranged from 1286 to 2662 μg $m^{-2} h^{-1}$, which was the highest N_2O emissions from permafrost region (Mu et al., 2017). The cumulative budget from permafrost region could reach 14 kg ha^{-1}, which indicated that permafrost region is likely to be a source of N_2O to the atmosphere (Marushchak et al., 2011; Repo et al., 2009).

Compared with those in other studies in the global scale, the N_2O flux we measured from the Daxing'an Mountains were located in the intermediate range for permafrost ecosystems. The highest rates of N_2O emission from the Daxing'an Mountains in our study were higher than those from permafrost region in the Skalluvaara (−0.88 to

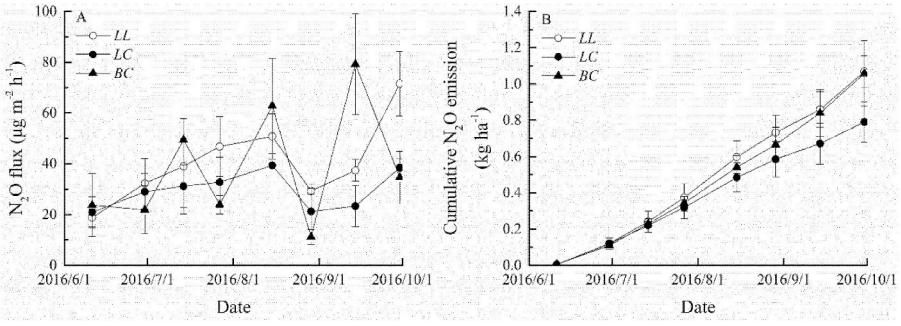

Fig. 2. N_2O fluxes (A) and cumulative N_2O emissions (B) from three types of swamp forests in the Daxing'an Mountains, northeast China. Swamp forest types were *Larix gmelinii - Ledum palustre var. dilatatum* (*LL*), *Larix gmelinii - Carex appendiculata* (*LC*) and *Betula fruticose - Carex schmidtii* (*BC*). (mean ± SD).

Table 2
N_2O emission and cumulative N_2O emissions from the three types of swamp forests in the Daxing'an Mountains, northeast China. (mean ± SD).

Plots	N_2O emission (μg $m^{-2} h^{-1}$)	Minimum–Maximum (μg $m^{-2} h^{-1}$)	Length of growing season (day)	Cumulative N_2O emissions (kg ha^{-1})	CV (%)
LL	40.74 ± 15.98a	18.82–71.57	111	1.07 ± 0.09a	40.74
LC	29.54 ± 7.28a	20.86–39.41	111	0.79 ± 0.18a	29.54
BC	38.34 ± 23.42a	11.81–79.25	111	1.05 ± 0.11a	38.35

The different lowercase letters within a column indicate significant differences ($P < 0.05$) among types of swamp forests at the Daxing'an Mountains, northeast China. Swamp forest types were *Larix gmelinii - Ledum palustre var. dilatatum* (*LL*), *Larix gmelinii - Carex appendiculata* (*LC*) and *Betula fruticose - Carex schmidtii* (*BC*). CV = coefficient of variation.

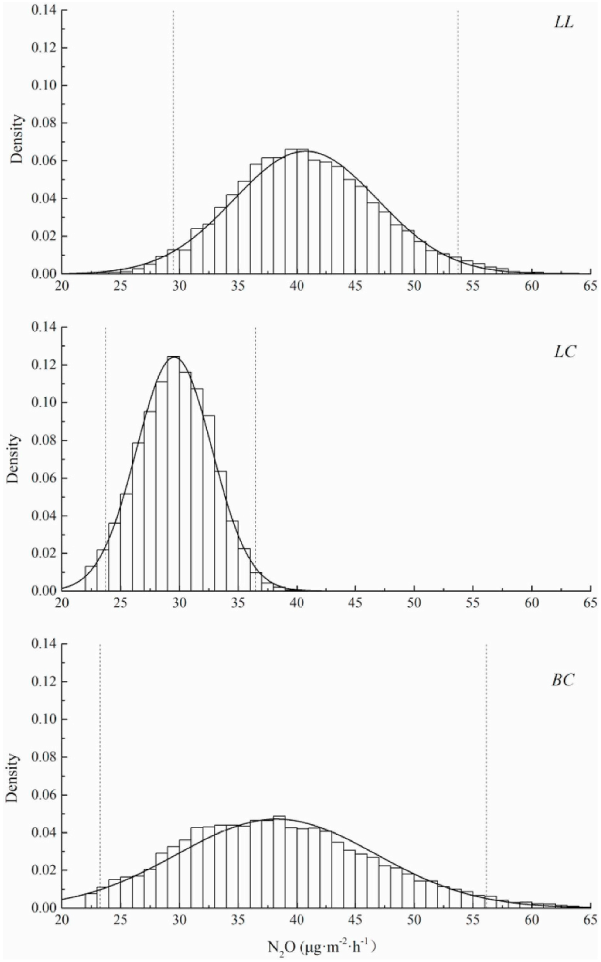

Fig. 3. Bootstrapped distribution of mean N_2O fluxes from three swamp forests in the Daxing'an Mountains, northeast China. Measured fluxes from all samples were randomly selected with replacement and a mean value calculated. Means were re-sampled in 10000 iterations. The solid line depicts a normal distribution, whereas the dotted vertical lines bracket 95% of the means calculated from the normal distributions. Swamp forest types were *Larix gmelinii - Ledum palustre var. dilatatum* (*LL*), *Larix gmelinii - Carex appendiculata* (*LC*) and *Betula fruticose - Carex schmidtii* (*BC*).

0.44 μg $m^{-2} h^{-1}$) (Palmer and Horn, 2012), Garwood Valley Antarctic region (0.6–6.0 μg $m^{-2} h^{-1}$) (Gregorich et al., 2006), Ny-Ålesund (−6.5–10.8 μg $m^{-2} h^{-1}$) (Zhu et al., 2012), Daxing'an Mountain (−14.21 to 13.09 μg $m^{-2} h^{-1}$) (Cui et al., 2018) and Qinghai-Tibetan Plateau (−22.35 to 14.05 μg $m^{-2} h^{-1}$) (Chen et al., 2017), but lower than those from the permafrost in Northeast European Russia (0.21–91.63 μg $m^{-2} h^{-1}$) (Voigt et al., 2017a), Eastern Siberia (−5.34–578.29 μg $m^{-2} h^{-1}$) (Takakai et al., 2008), Subarctic East European tundra (79.17–1291.67 μg $m^{-2} h^{-1}$) (Repo et al., 2009), Eboling mountain (1286–2662 μg $m^{-2} h^{-1}$) (Mu et al., 2017), Komi

Table 3
Pearson's correlation coefficients between the N_2O fluxes and environmental factors in the three swamp forests in the Daxing'an Mountains, northeast China.

Plots	ST	WTL	pH	NH_4^+-N	NO_3^--N	TOC	TN	C/N
LL	0.21	−0.42	0.34	−0.37	−0.77[a]	−0.05	0.42	−0.53
LC	0.44	0.37	0.28	0.00	−0.49	−0.10	0.41	−0.39
BC	0.35	0.36	−0.28	−0.10	−0.16	−0.14	0.00	−0.16

[a] Indicates significant effects at $P < 0.05$. ST, soil temperature; WTL, water table level; NH_4^+-N, ammonium nitrogen; NO_3^--N, nitrate nitrogen; TOC, total organic carbon; TN, total nitrogen; C/N, carbon-to-nitrogen ratio. Swamp forest types were *Larix gmelinii - Ledum palustre var. dilatatum* (*LL*), *Larix gmelinii - Carex appendiculata* (*LC*) and *Betula fruticose - Carex schmidtii* (*BC*).

Republic (−25–1308 μg $m^{-2} h^{-1}$) and Utsjoki (−3–683 μg $m^{-2} h^{-1}$) (Marushchak et al., 2011). The mean N_2O flux were higher than those from permafrost region in the Canadian Cryosols site (−4.75 and 25.34 μg $m^{-2} h^{-1}$) (Paré and Bedard-Haughn, 2012) and Eagle Plains (4.14–7.56 μg $m^{-2} h^{-1}$) (Köster et al., 2017), and lower than the Alexandra Fiord (109.3 μg $m^{-2} h^{-1}$) (Lamb et al., 2011). Our results are closest to the release of N_2O in the sub-Arctic tundra (4.16–141.67 μg $m^{-2} h^{-1}$), which were similar to mean N_2O flux as measured in our study (Gil et al., 2017).

The cumulative N_2O emissions varied in the range 0.79–1.07 kg ha^{-1} during the growing season in the permafrost region of Daxing'an Mountains. Permafrost region has been reported as a source of N_2O emissions (Marushchak et al., 2011; Repo et al., 2009). In previous studies, the N_2O flux from bare permafrost peatland was mainly from the soil to the atmosphere and was as high as 9–14 kg ha^{-1} (Marushchak et al., 2011; Repo et al., 2009; Takakai et al., 2008), which is more than 8 times the largest flux that we measured. In vegetated permafrost region, the highest cumulative N_2O reported was 2.67 kg ha^{-1}, which was more than twice our results (Takakai et al., 2008). Repo et al. (2009) estimated that the global N_2O emissions derived from bare peat sources was 0.1 Tg yr^{-1}, which accounted for 0.6% of the global annual N_2O emissions. Our results confirm those from previous studies showing that permafrost region is a potential source of N_2O flux (Marushchak et al., 2011; Repo et al., 2009; Takakai et al., 2008). On the other hand, vegetated soils in permafrost region showed negligible N_2O emissions or very low cumulative N_2O emission, which indicates these systems are weak sources, and could be sinks of N_2O emissions (Cui et al., 2018; Ma et al., 2007; Palmer and Horn, 2012; Voigt et al., 2017a; Zhu et al., 2012). Comparatively, the cumulative N_2O emissions that we measured in the Daxing'an Mountains were in the intermediate range of those from permafrost ecosystems.

In the permafrost region, most ecosystems were primarily limited by low soil N availability (Nordin et al., 2004; Wild et al., 2013). It has been shown low released of N_2O from N conservative permafrost soils (Palmer and Horn, 2012). N_2O emissions are mostly negligible from vegetated permafrost surfaces (Chen et al., 2017; Köster et al., 2017; Ma et al., 2007; Palmer and Horn, 2012; Zhu et al., 2012). Conversely, high N_2O emissions mostly occur from bare surfaces at the peatland (Marushchak et al., 2011; Repo et al., 2009). Furthermore, there is large

Table 4
The stepwise multiple linear regression model between N_2O flux and environmental factors in the three types of swamp forests in the Daxing'an Mountains, northeast China.

Plot	Regression model								R^2	P
	Intercept	ST	WTL	pH	NH_4^+-N	NO_3^--N	TOC	C/N		
LL	−323.79**		−0.62*	81.57***	2.31$^+$	−41.48***			0.7389	< 0.001
LC	121.31$^+$	5.67**				−72.98***	−2.594$^+$	7.385	0.6241	< 0.001
BC	21.755$^+$		2.72*			−62.73*	−2.536	9.357	0.4905	< 0.05

$^+$: indicates significant effects at $P < 0.1$; *: indicates significant effects at $P < 0.05$; **: indicates significant effects at $P < 0.01$; ***: indicates significant effects at $P < 0.001$. ST, soil temperature; WTL, water table level; NH_4^+-N, ammonium nitrogen; NO_3^--N, nitrate nitrogen; TOC, total organic carbon; C/N, carbon-to-nitrogen ratio. Swamp forest types were *Larix gmelinii - Ledum palustre var. dilatatum* (*LL*), *Larix gmelinii - Carex appendiculata* (*LC*) and *Betula fruticose - Carex schmidtii* (*BC*).

spatial variation of N_2O emissions from bare and vegetated soils. The NH_4^+-N (65 ± 99 μg g^{-1}) and NO_3^--N (51 ± 78 μg g^{-1}) of bare peat has been shown to be one order of magnitude higher than at a vegetated site (Marushchak et al., 2011). The high NH_4^+-N and NO_3^--N are available for soil microbes, and thus, for N_2O production. Plants significantly affect the differences in mineral nitrogen between bare and vegetated surfaces. Plants uptake mineral nitrogen from soil, reduce the supply of mineral nitrogen to microbes, and consequently reduce N_2O emissions.

High mineral nitrogen content in soil has been shown to stimulate "hot spots" of N_2O emissions. In the "N_2O hot spots" of the subarctic East European tundra, high N_2O emissions were released from bare soils where NO_3^--N in the bare peat circles (55 μg g^{-1}) was significantly higher than in vegetated surfaces (Repo et al., 2009). Mineral nitrogen has been considered to be the limiting factor for N_2O emissions from high-latitude permafrost ecosystems (Rodionow et al., 2006). In a previous study, Palmer and Horn (2012) reported that N_2O flux from nitrate-fertilized permafrost peat soil was significantly higher than from unfertilized permafrost peat soil. Different forms of N addition significantly facilitated N_2O flux from the permafrost region of the arctic lowland ecosystem (Ma et al., 2007). However, in the Qinghai-Tibet Plateau, N fertilizer additions had no significant effect on the rates of N_2O emissions when nitrogen was not limiting (Chen et al., 2017). Nevertheless, mineral nitrogen might be a key factor affecting N_2O emissions from permafrost. In our studies, the content of NH_4^+-N (4.22–5.04 mg kg^{-1}) and NO_3^--N (0.78–0.86 mg kg^{-1}) was significantly lower than in the bare surface soil of permafrost (Marushchak et al., 2011; Repo et al., 2009). Thus, low mineral nitrogen limited the rates of N_2O emissions from permafrost region in the Daxing'an Mountains (Cui et al., 2016).

4.2. The forest types had no significant effect on N_2O emissions

In our study, N_2O flux was consistently emitted from the swamp forest soils in the growing season (Fig. 2). The N_2O flux exhibited different seasonal variations pattern in the three swamp forests. The highest N_2O flux was observed on 30 September (71.57 μg m^{-2} h^{-1}) at *LL* plots, 15 August at *LC* plots (39.41 μg m^{-2} h^{-1}) and 14 September (79.25 μg m^{-2} h^{-1}) at *BC* plots, which were occur in the different period of growing season. The N_2O flux were determined by multiple environmental factors (Table 4). In the *LL* plots, the NH_4^+-N showed a gradual increasing trend from 14 July to the 30 September, while the NO_3^--N showed a gradual decreasing trend and had lowest content in the 30 September during the growing season. Besides, the water table level was the highest in the 14 September and sharply decrease to almost lowest level in the 30 September. The increased NH_4^+-N, decreased NO_3^--N and lower water table level probably significantly promoted the release of N_2O to the atmosphere in the 30 September. In the *LC* plots, the soil temperature was highest in the 15 August, which may be beneficial to microbial to use NO_3^--N and promote the production of N_2O flux. For the *BC* plots, the water table level was highest in the 14 September and suitable for denitrification, which is considered to be the main driver for the highest N_2O production.

During the growing season, the mean value of N_2O fluxes were 40.74 ± 15.98, 29.54 ± 7.28 and 38.34 ± 23.42 μg m^{-2} h^{-1} from *LL*, *LC* and *BC* plots, respectively (Table 1). The bootstrap estimates of N_2O emissions ranged from 29.47 to 53.73 μg m^{-2} h^{-1} (*LL* plots), from 23.00 to 35.55 μg m^{-2} h^{-1} (*LC* plots) and from 23.25 to 56.15 μg m^{-2} h^{-1} (*BC* plots) in the three swamp forests (Fig. 3). The mean N_2O emissions from the three swamp forests we investigated (40.76 ± 6.13, 29.56 ± 3.21 and 38.27 ± 8.46 μg m^{-2} h^{-1}, respectively) had the same value as data before bootstrapping (Fig. 3). The distributions of N_2O fluxes from the three swamp forests had no significant difference with regards to central tendency. In short, the forest types had no significant effect on N_2O emissions from swamp forests in the permafrost region of the Daxing'an Mountains.

In previous studies of permafrost, significant differences were shown between the N_2O emission from bare surface and those from vegetated soils (Marushchak et al., 2011; Repo et al., 2009). The contents of NH_4^+-N and NO_3^--N in these studies were higher in the bare surfaces than in the vegetated soils, which was mainly because the lack of plants resulted in increased mineral N (Marushchak et al., 2011; Repo et al., 2009). The high mineral N supported high N_2O production via nitrification and denitrification from the bare surfaces (Marushchak et al., 2011; Repo et al., 2009). In vegetated permafrost soils, the N_2O emissions have been shown to be mainly so low that they could be neglected (Chen et al., 2017; Cui et al., 2018; Köster et al., 2017; Ma et al., 2007; Palmer and Horn, 2012; Repo et al., 2009; Voigt et al., 2017a; Wang et al., 2014; Zhu et al., 2012).

Repo et al. (2009) and Wang et al. (2014) showed that there was no significant difference in N_2O emissions from sites with different types of plants. In the arctic, the NO_3^--N concentrations in all vegetated surfaces were low and limited the N_2O emissions produced by denitrification (Marushchak et al., 2011; Repo et al., 2009). In the Daxing'an Mountains, nitrification might be the dominant process that produces N_2O because the vegetated soils had high NH_4^+-N (49.1–343.8 mg kg^{-1}) (Wang et al., 2014). However, it is very likely that the changes of nutrient availability affected the activities of soil microbes and enzymes in the N cycling (Wang et al., 2014). In our studies, the NH_4^+-N content was 4.38 ± 2.03, 5.14 ± 1.52 and 4.22 ± 1.84 mg kg^{-1}, meanwhile NO_3^--N content was 0.86 ± 0.33, 0.78 ± 0.33 and 0.80 ± 0.22 mg kg^{-1} in the *LL*, *LC* and *BC* plots, respectively. Thus, all three types of swamp forests had low NH_4^+-N and NO_3^--N contents and these were not significantly different; all significantly limited the N_2O emissions. Therefore, N_2O emissions from the permafrost swamp forests were controlled by the availability of mineral nitrogen and there were no significant differences between them.

4.3. N_2O emissions as affected by nitrate nitrogen in the permafrost region

The processes affecting production and consumption of N_2O are complex. N_2O is mainly produced by two microbial processes in soil:

Table 5
Comparison of studies that reported N_2O fluxes from in-situ permafrost region.

Location	Latitude and longitude	Ecosystem type	Soil moisture (%)	Water table level (cm)	N_2O fluxes ($\mu g\ m^{-2} h^{-1}$)		Cumulative N_2O emissions ($kg\ ha^{-1}$)	Community	Measurement period	Reference
					Mean	Range				
Daxing'an Mountains	53°28′N, 122°20′E	Swamp forest		−13.14 ± 10.65	40.76	18.82–71.57	1.07	*Larix gmelinii*, *Ledum palustre var. dilatatum*, *Betula platyphylla*, *Betula fruticose*, *Vaccinium uliginosum* and *Vaccinium vitis-idaea*	Growing season	This study
Daxing'an Mountains	53°28′N, 122°20′E	Swamp forest		−1.87 ± 4.87	29.56	20.86–39.41	0.79	*Larix gmelinii*, *Carex appendiculata*, *Betula platyphylla*, *Betula fruticose* and *Alnus sibirica*	Growing season	This study
Daxing'an Mountains	53°28′N, 122°20′E	Swamp forest		+2.59 ± 5.14	38.27	11.81–79.25	1.05	*Betula fruticose* and *Carex schmidtii*	Growing season	This study
Garwood Valley, Antarctic	78°01′S, 163°53′E	Lake edge	35–65			0.6–6		Bare	Summer	Gregorich et al. (2006)
Devon Island, Canada	75°40′N 84°35′W	Lowland	20 ± 5				0.49×10^{-3}–0.93×10^{-3}	Bare	16 June to July 13	Ma et al. (2007)
			66 ± 29				0.17×10^{-3}–2.58×10^{-3}	*Alectoria* sp. and *Eriophorum* sp.		
			648 ± 246				-0.03×10^{-3}–7.18×10^{-3}	*Carex membranacea* and *Carex stans*		
Eastern Siberia, Russia	62°19′N, 129°30′E	Forests	3–52[a]			−0.47–7.23	0.015–0.043	*Larix cajanderi* and *Vaccinium vitiidaea*	Growing season	Takakai et al. (2008)
		Dry grassland	11–39[a]			0.16–10.84	0.057–0.204	*Elytrigia repens*		
		Wet grassland	15–100[a]			37.71–578.29	−0.039–2.671	*Carex orthostachys* and *Glyceria lithuanica*		
		Pond surface	100[a]	−40.33–1.26[a]		−5.34–2.98	−0.053 to −0.027	No vegetation pond surface		
Subarctic East European tundra	67.03° N, 62.57° E	Peat circles	64 ± 1	−18 ± 7		79.17–1291.67	9–14	Bare	Growing season	Repo et al. (2009)
		Plateau vegetation	16 ± 1	−35 ± 2			0[a]	*Ledum decumbens* and *Rubus chamaemorus*		
		Sphagnum depressions	43 ± 5	−15 ± 3			0[a]	*Ledum decumbens* and *Rubus chamaemorus*		
		Fen		1 ± 4			0[a]	*Carex aquatilis*		
		Upland	19 ± 3	−29 ± 5			0[a]	*Betula nana* and *Salix* sp.		
Alexandra Fiord, Canada	78°53′N, 75°46′W	Tundra			109.3			*Vaccinium uliginosum*, *Cassiope tetragona*, *Carex misandra* and *Luzula arctica*	Mid-July	Lamb et al. (2011)
Komi Republic, Russia	67°03′N, 62°57′E	Peat circles	70 and 76	−20 and −17	337.5 and 421.3	108–1308	14	Bare	Growing season	Marushchak et al. (2011)
		Peat mounds	19 ± 2		45	0–133	0	Bare		
		Peat plateau	27 and 30	−26 and −24	1.67 and 2.5	−25–17	0	*Ledum decumbens*, *Rubus chamaemorus* and *Vaccinium uliginosum*		
		Fen		−2	−2.5 and 0	−25–17	0	Sphagnum mat		
		Tundra heath	14 and 18	−30	−0.42 and 0.42	−25–17	0	*Pleurozium schreberi*, *Drepanocladus aduncus* and *Sphagnum* sp		
Utsjoki, Northern Finland	69°35′N, 26°12′E	Bare palsas	33 ± 15		108.33	16–683		Bare		
		Vegetated palsas	17 ± 9		8.33	−3–32		*Betula nana* and *Salix* sp.		
		Frost boils	68 ± 9		0	−6–4		Bare		

(*continued on next page*)

Table 5 (*continued*)

Location	Latitude and longitude	Ecosystem type	Soil moisture (%)	Water table level (cm)	N_2O fluxes (μg $m^{-2} h^{-1}$)		Cumulative N_2O emissions (kg ha^{-1})	Community	Measurement period	Reference
					Mean	Range				
Skalluvaara, northwestern Finnish	69°49′13″N, 27°9′47″E	Palsa peat	74 ± 0.3		Approximate 0[a]	−0.88–0.44		*Rubus chamaemorus*, *Vaccinium myrtillus*, *Vaccinium vitis-idea*, *Vaccinium uliginosum*, *Empetrum nigrum*, *Rhododendron tomentosum*, *Cornus suecica*, *Sphagnum fallax*, *Sphagnum riparium*, *Betula pubescens* subsp. *czerepanovii* and *Betula nana*.	July	Palmer and Horn (2012)
Churchill, Canada	58° 45′N; 93° 51′W	Tundra	10–550		−4.75			*Dryas integrifolia*	Growing season	Paré and Bedard-Haughn (2012)
Daring Lake, Canada	64°E 50′N; 111°E 38′W	Esker	50–230		25.34			*Empetrum nigrum*, *A. alpine*, *B. glandulosa*, *Carex* spp. and *Eriophorium vaginatum*		
Truelove lowland, Canada	75°E 33′N; 84°E 40′W	Beach	60–220					*Dryas integrifolia* and *Cassiope tetragona*		
Ny-Ålesund, Svalbard	79°55′N, 11°56′E	Tundra I	11.5–43.5		8.3 ± 13.2			*Salix polaris*, *Cerastium arcticum*, and *Drepanocladus* spp	Summer	Zhu et al. (2012)
		Tundra II	27.9–50.0		2.6 ± 1.2	−6.5–10.8		*Salix polaris*, *Cerastium arcticum*, and *Drepanocladus* spp		
Subarctic tundra	67°03′N, 62°57′E	Peat	46–75		33.33	4.16–141.67		Bare	Growing season	Gil et al. (2017)
Eagle Plains, Canada Tsiigehtchic, Canada	66°22′N,136°43′W 67°26′N,133°45′W	Forest	54.9		4.14–7.56[a]			*Picea mariana* (Mill.) BSP and *Picea glauca* (Moench) Voss	Summer	Köster et al. (2017)
Qinghai-Tibetan Plateau, China	34°43′43.9″N, 92°53′45.3″E	Alpine meadow	8.5–30.8[a]		1.74 ± 0.83	−22.35–14.05[a]		*Kobresia pygmaea*, *Kobresia humilis* Sergievskaja, *Kobresia capillifolia*, *Kobresia myosuroides* Fiori, *Kobresia graminifolia*, *Carex atrofusca Schkuhr* subsp., and *Carex scabriostris*	Growing season	Chen et al. (2017)
Eboling Mountain, China	38.00°N, 100.91°E	Thermokarst	130.9 ± 10.6			1286–2662[a]		*Carex* L. and *Kobresia Willd*	Growing-season	Mu et al. (2017)
Northeast European Russia	67°03′N, 62°55′E	Bare peat	26–35	−33 to −32	19.71	0.21–91.63[a]	0.21 and 0.78[a]	Bare	Growing season	Voigt et al. (2017a,b)
		Peat plateau	16–17	−29 to −25	Approximate 0	−0.81–3.07[a]	0 and 0.02[a]	*Ledum decumbens* and *Rubus chamaemorus* L.		
		Upland Tundra	11–17	−59 to −45	Approximate 0		−0.04 and 0[a]	*Betula nana* L., *Vaccinium uliginosum* L., *Salix* sp., *Empetrum nigrum* subsp. *hermaphroditum*		
Great Hing' an Mountains, Northeastern China	52°94′N, 122°86′E	Peatland	8.62–78.41		1.87 ± 1.34	−14.21–10.78[a]	0.06[a]	*Betula fruticosa* and *Sphagnum mosses*	Growing season	Cui et al. (2018)
		Peatland	2.80–90.55		2.66 ± 0.36	−11.52–13.09[a]	0.08[a]	*Ledum palustre* and *Sphagnum mosses*		

[a] Indicates the data were extracted from a digitized figure in the original article. The units of N_2O fluxes were converted to μg $m^{-2} h^{-1}$, the units of cumulative N_2O emissions were converted to kg ha^{-1}, the units of soil moisture were converted to %.

nitrification (the oxidation of ammonium to nitrite and nitrate) and denitrification (the reduction of nitrate and nitrite to nitric oxide, nitrous oxide, and dinitrogen) (Richardson et al., 2009). Many environmental factors have been reported to affect microbially mediated N_2O emissions from soil in the permafrost region to the atmosphere, such as air temperature, soil temperature, water table level, soil moisture, precipitation, pH, NH_4^+-N, NO_3^--N, TOC, gross N mineralization, N content and C/N ratio (Chen et al., 2017; Cui et al., 2018; Gil et al., 2017; Ma et al., 2007; Marushchak et al., 2011; Paré and Bedard-Haughn, 2012).

Soil moisture is an important determinant of microbial activity exerting dominant control over O_2 availability, which would control the released of N_2O flux through the redox conditions in the soil. Marushchak et al. (2011) reported that N_2O emissions from peat circles (ranged from 2.6 to 31.4 mg N_2O m^2 day^{-1}) were negative correlation with WFPS (with mean 76% and 70% in 2007 and 2008) and a positive correlation with water table level at Seida site, which indicate that N_2O production at these surfaces can be limited by excessive soil moisture and dominated by denitrification. The high bulk density intermediate soil moisture (64%) in the peat circles of subarctic creates both aerobic and anaerobic microenvironments that allow simultaneous aerobic nitrification and anaerobic denitrification to take place (Repo et al., 2009). Stable isotope analysis indicated that at 50–55% water filled pore space (incubated at WFPS representative of the field), nitrification was the dominant (> 80%) N_2O emitting process (Ma et al., 2007). At low soil moisture (less than 30%), moisture could explain 9% of seasonal variation of N_2O fluxes (Chen et al., 2017). Although there was no significant correlation between N_2O flux and soil moisture (less than 30%) at raised beach crest, N_2O flux with soil moisture less than field capacity (60–65%) are predominantly produced nitrification (Ma et al., 2007). Soil moisture showed a weak correlation with N_2O fluxes from Daxing'an Mountains, but it is not clear that the N_2O flux was released from nitrification or denitrification (Cui et al., 2018).

Soil moisture can control the availability of O_2, which directly determines the microbial community structure and the nitrification and denitrification processes (Gleeson et al., 2010). In our study, the mean water table level was 13.14 ± 10.65 cm below the soil surface in the *LL* plots, which had the similar water table level as the subarctic peatland (Marushchak et al., 2011; Repo et al., 2009). In this water table level condition, N_2O emissions were weak positive correlated with NH_4^+-N and significant negatively correlated with water table level and NO_3^--N, which indicated that *LL* plots could simultaneously perform aerobic nitrification and anaerobic denitrification (Repo et al., 2009). This means that simultaneously nitrification and denitrification was the potential source of N_2O fluxes in the *LL* plots.

The mean water table levels of *LC* and *BC* plots were −1.87 ± 4.87 cm and 2.59 ± 5.14 cm (i.e. above the soil surface); these were significantly higher than was the water table in the *LL* plots. The soil in *LC* and *BC* plots was completely saturated and this condition created an anaerobic environment for microorganisms. The N_2O had a weaker negative correlation with NO_3^--N ($P > 0.05$) in these two plots than in *LL* plots, and the stepwise multiple linear regression analysis showed that denitrification was affected by NO_3^--N on the temporal variability on N_2O emissions in the permafrost at these sites. These results also implied that denitrification was also dominant in the *LC* and *BC* plots, but this must be confirmed by future studies. The N_2O emission was affected by soil temperature, water table level, pH, NH_4^+-N, NO_3^--N, TOC and C/N in the three swamp forests in Daxing'an Mountains. The stepwise multiple linear regression analysis showed that together, multiple environment factors could explain 73.89%, 62.41% and 49.05% of the temporal variability of N_2O emission fluxes in *LL*, *LC* and *BC* plots, respectively (Table 4). However, the soil factors that significantly affected N_2O emissions were different in the different types of swamp forest.

In the *LL* plots, the N_2O emissions were mainly derived from nitrification and denitrification, and water table level, pH, NH_4^+-N and NO_3^--N significantly affected the N_2O emissions. The N_2O emissions was positively correlated with NH_4^+-N ($P < 0.1$) and negative correlated with water table level ($P < 0.05$), which implied that NH_4^+-N and water table level was encouraged microbes via nitrification and enhanced N_2O emissions. The NO_3^--N was significant negative correlated with N_2O emissions ($P < 0.001$), denitrification also played an important role in N_2O release. However, the pH of the *LL* plots was acidic, which affected the activity of the denitrifying microorganisms; low pH is known to restrict the denitrifying activity of soils.

The *LC* and *BC* plots experienced the same influence of NO_3^--N, TOC and C/N ratio. Denitrification is a heterotrophic process and requires a C source for energy. The TOC at these sites was consumed as energy to produce N_2O. The C/N ratio was positively correlated with N_2O emissions, but the relationship was not significant ($P > 0.1$). Thus C/N ratio had only a weak influence on the N_2O release. Soil temperature was found to be one of the key factors influencing N_2O emissions from *LC* plots. In the *LC* plots, the mean soil temperature was 8.02 ± 2.95 °C (ranging from 3.62 °C to 11.87 °C), which was below the critical level and resulted in the positive effect on N_2O production. In the *BC* plots, the NO_3^--N was negative correlated with N_2O emissions ($P < 0.05$), may be resulting in a rapid depletion of the available soil NO_3^--N pool via denitrification.

5. Conclusions

(1) During the growing season, significant N_2O emissions are released from swamp forest soil in permafrost to the atmosphere. In this study, these emissions ranged from 11.81 to 79.25 μg m^{-2} h^{-1} and the cumulative N_2O emissions were estimated to be 0.79–1.07 kg ha^{-1}. On a global scale of N_2O emissions, N_2O fluxes from the permafrost forest swamp ecosystems of the Daxing'an Mountains are in the intermediate range.

(2) In this study, the mean values of N_2O fluxes were 40.76, 29.56 and 38.27 μg m^{-2} h^{-1} from *LL*, *LC* and *BC* swamp forest types, respectively. The types of swamp forest in the permafrost region of the Daxing'an Mountains have no significant effect on the N_2O emissions.

(3) N_2O emissions from swamp forest soil in permafrost region can be influenced by soil temperature, water table level, pH, ammonium nitrogen, nitrate nitrogen, TOC and C/N ratio. Nitrate nitrogen in these swamp forest systems is a significant influence on the temporal variability of N_2O emission. Denitrification is a potential source of N_2O fluxes in permafrost region of the Daxing'an Mountains.

Acknowledgement

This work was supported by the National Natural Science Foundation of China (No.31870471, 31470543). We are sincerely grateful to Heilongjiang Mohe Forest Ecosystem Research Station.

Appendix A. Supplementary data

Supplementary data to this article can be found online at https://doi.org/10.1016/j.atmosenv.2018.10.045.

References

Alves, B.J.R., Smith, K.A., Flores, R.A., Cardoso, A.S., Oliveira, W.R.D., Jantalia, C.P., Urquiaga, S., Boddey, R.M., 2012. Selection of the most suitable sampling time for static chambers for the estimation of daily mean N_2O flux from soils. Soil Biol. Biochem. 46, 129–135.

Bengtsson, G., Bengtson, P., Mansson, K.F., 2003. Gross nitrogen mineralization-, immobilization-, and nitrification rates as a function of soil C/N ratio and microbial activity. Soil Biol. Biochem. 35, 143–154.

Bremner, J.M., Mulvaney, C.S., 1982. Nitrogen - Total. American Society of Agronomy, New York, U.S.A.

Butterbach-Bahl, K., Baggs, E.M., Dannenmann, M., Kiese, R., Zechmeister-Boltenstern, S.,

2013. Nitrous oxide emissions from soils: how well do we understand the processes and their controls? Philos T R Soc B 368, 20130122.
Camill, P., 2005. Permafrost thaw accelerates in boreal peatlands during late-20th century climate warming. Climatic Change 68, 135–152.
Castaldi, S., Bertolini, T., Valente, A., Chiti, T., Valentini, R., 2013. Nitrous oxide emissions from soil of an African rain forest in Ghana. Biogeosciences 10, 4179–4187.
Chen, S.Y., Liu, W.J., Qin, X., Liu, Y.S., Zhang, T.Z., Chen, K.L., Hu, F.Z., Ren, J.W., Qin, D.H., 2012. Response characteristics of vegetation and soil environment to permafrost degradation in the upstream regions of the Shule River Basin. Environ. Res. Lett. 7, 189–190.
Chen, X.P., Wang, G.X., Zhang, T., Mao, T.X., Wei, D., Hu, Z.Y., Song, C.L., 2017. Effects of warming and nitrogen fertilization on GHG flux in the permafrost region of an alpine meadow. Atmos. Environ. 157, 111–124.
Cheng, G.D., Jin, H.J., 2013. Permafrost and groundwater on the Qinghai-Tibet Plateau and in Northeast China. Hydrogeol. J. 21, 5–23.
Cheng, G.D., Wu, T.H., 2007. Responses of permafrost to climate change and their environmental significance, Qinghai-Tibet Plateau. J Geophys Res-Earth 112, F02S03.
Cui, Q., Song, C.C., Wang, X.W., Shi, F.X., Wang, L.L., Guo, Y.D., 2016. Rapid N_2O fluxes at high level of nitrate nitrogen addition during freeze-thaw events in boreal peatlands of Northeast China. Atmos. Environ. 135, 1–8.
Cui, Q., Song, C.C., Wang, X.W., Shi, F.X., Yu, X.Y., Tan, W.W., 2018. Effects of warming on N_2O fluxes in a boreal peatland of Permafrost region, Northeast China. Sci. Total Environ. 616–617, 427–434.
Ding, W.X., Cai, Y., Cai, Z.C., Yagi, K., Zheng, X.H., 2007. Nitrous oxide emissions from an intensively cultivated maize-wheat rotation soil in the North China Plain. Sci. Total Environ. 373, 501–511.
Dobbie, K.E., Smith, K.A., 2006. The effect of water table depth on emissions of N_2O from a grassland soil. Soil Use Manag. 22, 22–28.
Du, R., Lu, D.R., Wang, G.C., 2006. Diurnal, seasonal, and inter-annual variations of N_2O fluxes from native semi-arid grassland soils of inner Mongolia. Soil Biol. Biochem. 38, 3474–3482.
Elberling, B., Christiansen, H.H., Hansen, B.U., 2010. High nitrous oxide production from thawing permafrost. Nat. Geosci. 3, 332–335.
Frey, K.E., McClelland, J.W., 2009. Impacts of permafrost degradation on arctic river biogeochemistry. Hydrol. Process. 23, 169–182.
Gil, J., Pérez, T., Boering, K., Martikainen, P.J., Biasi, C., 2017. Mechanisms responsible for high N_2O emissions from subarctic permafrost peatlands studied via stable isotope techniques. Global Biogeochem. Cycles 31, 172–189.
Gleeson, D.B., Müller, C., Banerjee, S., Ma, W., Siciliano, S.D., Murphy, D.V., 2010. Response of ammonia oxidizing archaea and bacteria to changing water filled pore space. Soil Biol. Biochem. 42, 1888–1891.
Gregorich, E.G., Hopkins, D.W., Elberling, B., Sparrow, A.D., Novis, P., Greenfield, L.G., Rochette, P., 2006. Emission of CO_2, CH_4 and N_2O from lakeshore soils in an Antarctic dry valley. Soil Biol. Biochem. 38, 3120–3129.
Harden, J.W., Koven, C.D., Ping, C.L., Hugelius, G., David McGuire, A., Camill, P., Jorgenson, T., Kuhry, P., Michaelson, G.J., O'Donnell, J.A., Schuur, E.A.G., Tarnocai, C., Johnson, K., Grosse, G., 2012. Field information links permafrost carbon to physical vulnerabilities of thawing. Geophys. Res. Lett. 39, L15704.
Hugelius, G., Strauss, J., Zubrzycki, S., Harden, J.W., Schuur, E.A.G., Ping, C.L., Schirrmeister, L., Grosse, G., Michaelson, G.J., Koven, C.D., O'Donnell, J.A., Elberling, B., Mishra, U., Camill, P., Yu, Z., Palmtag, J., Kuhry, P., 2014. Estimated stocks of circumpolar permafrost carbon with quantified uncertainty ranges and identified data gaps. Biogeosciences 11, 6573–6593.
Hutchinson, G.L., Livingston, G.P., Healy, R.W., Striegl, R.G., 2000. Chamber measurement of surface-atmosphere trace gas exchange: numerical evaluation of dependence on soil, interfacial layer, and source/sink properties. J. Geophys. Res. Atmos. 105, 8865–8875.
IPCC, 2013. Climate Change 2013: the Physical Science Basis: Working Group I Contribution to the Fifth Assessment Report of the Intergovernmental Panel on Climate Change. Cambridge University Press, Cambridge, UK, and New York.
Jin, H.J., Yu, Q.H., Lii, L.Z., Guo, D.X., He, R.X., Yu, S.P., Sun, G.Y., Li, Y.W., 2007. Degradation of permafrost in the Xing'anling Mountains, northeastern China. Permafrost Periglac 18, 245–258.
Kiese, R., Hewett, B., Graham, A., Butterbach-Bahl, K., 2003. Seasonal variability of N_2O emissions and CH_4 uptake by tropical rainforest soils of Queensland, Australia. Global Biogeochem. Cycles 17, 13.
Köster, E., Koster, K., Berninger, F., Aaltonen, H., Zhou, X., Pumpanen, J., 2017. Carbon dioxide, methane and nitrous oxide fluxes from a fire chronosequence in subarctic boreal forests of Canada. Sci. Total Environ. 601–602, 895–905.
Lamb, E.G., Han, S., Lanoil, B.D., Henry, G.H.R., Brummell, M.E., Banerjee, S., Siciliano, S.D., 2011. A High Arctic soil ecosystem resists long-term environmental manipulations. Global Change Biol. 17, 3187–3194.
Lang, H.Q., 1999. Wetland Vegetation in China (In Chinese). Science Press, Beijing, China.
Li, Y.Y., Dong, S.K., Liu, S.L., Zhou, H.K., Gao, Q.Z., Cao, G.M., Wang, X.X., Su, X.K., Zhang, Y., Tang, L., Zhao, H.D., Wu, X.Y., 2015. Seasonal changes of CO_2, CH_4 and N_2O fluxes in different types of alpine grassland in the Qinghai-Tibetan Plateau of China. Soil Biol. Biochem. 80, 306–314.
Ma, W.K., Schautz, A., Fishback, L.A.E., Bedard-Haughn, A., Farrell, R.E., Siciliano, S.D., 2007. Assessing the potential of ammonia oxidizing bacteria to produce nitrous oxide in soils of a high arctic lowland ecosystem on Devon Island, Canada. Soil Biol. Biochem. 39, 2001–2013.
Marushchak, M.E., Pitkamaki, A., Koponen, H., Biasi, C., Seppala, M., Martikainen, P.J., 2011. Hot spots for nitrous oxide emissions found in different types of permafrost peatlands. Global Change Biol. 17, 2601–2614.
Mu, C.C., Abbott, B.W., Zhao, Q., Su, H., Wang, S.F., Wu, Q.B., Zhang, T.J., Wu, X.D., 2017. Permafrost collapse shifts alpine tundra to a carbon source but reduces N_2O and CH_4 release on the northern Qinghai-Tibetan Plateau. Geophys. Res. Lett. 44, 8945–8952.
Nelson, D.W., Sommers, L.E., 1996. Total carbon, organic carbon, and organic matter. In: Sparks, D.L., Page, A.L., Helmke, P.A., Loeppert, R.H., Soltanpour, P.N., Tabatabai, M.A., Johnston, C.T., Sumner, M.E. (Eds.), Methods of Soil Analysis. Part 3. Chemical Methods. Soil Science Society of America Book Series, Wisconsin, pp. 961–1010.
Nordin, A., Schmidt, I.K., Shaver, G.R., 2004. Nitrogen uptake by arctic soil microbes and plants in relation to soil nitrogen supply. Ecology 85, 955–962.
Palmer, K., Biasi, C., Horn, M.A., 2012. Contrasting denitrifier communities relate to contrasting N_2O emission patterns from acidic peat soils in arctic tundra. ISME J. 6, 1058–1077.
Palmer, K., Horn, M.A., 2012. Actinobacterial nitrate reducers and proteobacterial denitrifiers are abundant in N_2O-metabolizing palsa peat. Appl. Environ. Microbiol. 78, 5584–5596.
Paré, M.C., Bedard-Haughn, A., 2012. Landscape-scale N mineralization and greenhouse gas emissions in Canadian Cryosols. Geoderma 189, 469–479.
Petersen, S.O., Ambus, P., Elsgaard, L., Schjønning, P., Olesen, J.E., 2013. Long-term effects of cropping system on N_2O emission potential. Soil Biol. Biochem. 57, 706–712.
Qin, S.P., Wang, Y.Y., Hu, C.S., Oenema, O., Li, X.X., Zhang, Y.M., Dong, W.X., 2012. Yield-scaled N_2O emissions in a winter wheat summer corn double-cropping system. Atmos. Environ. 55, 240–244.
Ravishankara, A.R., Daniel, J.S., Portmann, R.W., 2009. Nitrous oxide (N_2O): the dominant ozone-depleting substance emitted in the 21st century. Science 326, 123–125.
Repo, M.E., Susiluoto, S., Lind, S.E., Jokinen, S., Elsakov, V., Biasi, C., Virtanen, T., Martikainen, P.J., 2009. Large N_2O emissions from cryoturbated peat soil in tundra. Nat. Geosci. 2, 189–192.
Richardson, D., Felgate, H., Watmough, N., Thomson, A., Baggs, E., 2009. Mitigating release of the potent greenhouse gas N_2O from the nitrogen cycle - could enzymic regulation hold the key? Trends Biotechnol. 27, 388–397.
Rodionow, A., Flessa, H., Kazansky, O., Guggenberger, G., 2006. Organic matter composition and potential trace gas production of permafrost soils in the forest tundra in northern Siberia. Geoderma 135, 49–62.
Schuur, E.A.G., Vogel, J.G., Crummer, K.G., Lee, H., Sickman, J.O., Osterkamp, T.E., 2009. The effect of permafrost thaw on old carbon release and net carbon exchange from tundra. Nature 459, 556–559.
Shvaleva, A., Siljanen, H.M.P., Correia, A., Silva, F.C.E., Lamprecht, R.E., Lobo-do-Vale, R., Bicho, C., Fangueiro, D., Anderson, M., Pereira, J.S., Chaves, M.M., Cruz, C., Martikainen, P.J., 2015. Environmental and microbial factors influencing methane and nitrous oxide fluxes in Mediterranean cork oak woodlands: trees make a difference. Front. Microbiol. 6, 1104.
Siciliano, S.D., Ma, W.K., Ferguson, S., Farrell, R.E., 2009. Nitrifier dominance of Arctic soil nitrous oxide emissions arises due to fungal competition with denitrifiers for nitrate. Soil Biol. Biochem. 41, 1104–1110.
Song, C.C., Xu, X.F., Tian, H.Q., Wang, Y.Y., 2009. Ecosystem-atmosphere exchange of CH_4 and N_2O and ecosystem respiration in wetlands in the Sanjiang Plain, Northeastern China. Global Change Biol. 15, 692–705.
Song, C.C., Zhang, J.B., Wang, Y.Y., Wang, Y.S., Zhao, Z.C., 2008. Emission of CO_2, CH_4 and N_2O from freshwater marsh in northeast of China. J. Environ. Manag. 88, 428–436.
Szukics, U., Abell, G.C.J., Hodl, V., Mitter, B., Sessitsch, A., Hackl, E., Zechmeister-Boltenstern, S., 2010. Nitrifiers and denitrifiers respond rapidly to changed moisture and increasing temperature in a pristine forest soil. FEMS Microbiol. Ecol. 72, 395–406.
Takakai, F., Desyatkin, A.R., Lopez, C.M.L., Fedorov, A.N., Desyatkin, R.V., Hatano, R., 2008. CH_4 and N_2O emissions from a forest-alas ecosystem in the permafrost taiga forest region, eastern Siberia, Russia. J. Geophys. Res.-Biogeosci. 113, G02002.
Tang, X.L., Liu, S.G., Zhou, G.Y., Zhang, D.Q., Zhou, C.Y., 2006. Soil-atmospheric exchange of CO_2, CH_4, and N_2O in three subtropical forest ecosystems in southern China. Global Change Biol. 12, 546–560.
Verma, A., Tyagi, L., Yadav, S., Singh, S.N., 2006. Temporal changes in N_2O efflux from cropped and fallow agricultural fields. Agric. Ecosyst. Environ. 116, 209–215.
Voigt, C., Lamprecht, R.E., Marushchak, M.E., Lind, S.E., Novakovskiy, A., Aurela, M., Martikainen, P.J., Biasi, C., 2017a. Warming of subarctic tundra increases emissions of all three important greenhouse gases – carbon dioxide, methane, and nitrous oxide. Global Change Biol. 23, 3121–3138.
Voigt, C., Marushchak, M.E., Lamprecht, R.E., Jackowicz-Korczynski, M., Lindgren, A., Mastepanov, M., Granlund, L., Christensen, T.R., Tahvanainen, T., Martikainen, P.J., Biasi, C., 2017b. Increased nitrous oxide emissions from Arctic peatlands after permafrost thaw. P Natl Acad Sci USA 114, 6238–6243.
Wang, J.Y., Song, C.C., Zhang, J., Wang, L.L., Zhu, X.Y., Shi, F.X., 2014. Temperature sensitivity of soil carbon mineralization and nitrous oxide emission in different ecosystems along a mountain wetland-forest ecotone in the continuous permafrost of Northeast China. Catena 121, 110–118.
Wild, B., Schnecker, J., Barta, J., Capek, P., Guggenberger, G., Hofhansl, F., Kaiser, C., Lashchinsky, N., Mikutta, R., Mooshammer, M., Santruckova, H., Shibistova, O., Urich, T., Zimov, S.A., Richter, A., 2013. Nitrogen dynamics in turbic Cryosols from Siberia and Greenland. Soil Biol. Biochem. 67, 85–93.
Xu, R., Prentice, I.C., Spahni, R., Niu, H.S., 2012. Modelling terrestrial nitrous oxide emissions and implications for climate feedback. New Phytol. 196, 472–488.
Xu, R., Wang, Y.S., Zheng, X.H., Ji, B.M., Wang, M.X., 2003. A comparison between measured and modeled N_2O emissions from Inner Mongolian semi-arid grassland. Plant Soil 255, 513–528.
Xue, K., Yuan, M.M., Shi, Z.,J., Qin, Y.J., Deng, Y., Cheng, L., Wu, L.Y., He, Z.L., Van Nostrand, J.D., Bracho, R., Natali, S., Schuur, E.A.G., Luo, C.W., Konstantinidis, K.T.,

Wang, Q., Cole, J.R., Tiedje, J.M., Luo, Y.Q., Zhou, J.Z., 2016. Tundra soil carbon is vulnerable to rapid microbial decomposition under climate warming. Nat. Clim. Change 6, 595–600.

Yan, J.H., Zhang, W., Wang, K.Y., Qin, F., Wang, W.T., Dai, H.T., Li, P.X., 2014. Responses of CO_2, N_2O and CH_4 fluxes between atmosphere and forest soil to changes in multiple environmental conditions. Global Change Biol. 20, 300–312.

Yuan, M.M., Zhang, J., Xue, K., Wu, L., Deng, Y., Deng, J., Hale, L., Zhou, X., He, Z., Yang, Y., Van Nostrand, J.D., Schuur, E.A.G., Konstantinidis, K.T., Penton, C.R., Cole, J.R., Tiedje, J.M., Luo, Y., Zhou, J., 2018. Microbial functional diversity covaries with permafrost thaw-induced environmental heterogeneity in tundra soil. Global Change Biol. 24, 297–307.

Zhang, F.R., 2002. Soil Geography (In Chinese). China Agriculture Press, Beijing, China.

Zhu, R.B., Chen, Q.Q., Ding, W., Xu, H., 2012. Impact of seabird activity on nitrous oxide and methane fluxes from High Arctic tundra in Svalbard, Norway. J. Geophys. Res.-Biogeosci. 117, 1703–1705.